Characterization of Monostatic Base Stations Sensing Resolution Using 5G Reference Signals

Tanguy Ropitault*,†, Steve Blandino*,†, David Griffith‡, Anirudha Sahoo‡, Thao Nguyen‡, Nada Golmie‡

*Associates, CTL, National Institute of Standards and Technology, Gaithersburg, MD, USA
†Prometheus Computing LLC, Bethesda, MD, USA
‡CTL, National Institute of Standards and Technology, Gaithersburg, MD, USA

Email: {tanguy.ropitault, steve.blandino, david.griffith, anirudha.sahoo, thao.t.nguyen, nada.golmie}@nist.gov

Abstract—Sensing is poised to be a crucial feature in 6G, leading 3GPP to integrate sensing capabilities into the 5G New Radio (NR) framework. Significant progress has been made, but extensive work remains in defining architectures, protocol operations, and deployment strategies. Successful adoption by operators hinges on balancing cost-effectiveness with anticipated benefits. We introduce a novel architecture that repurposes existing 3GPP signals—Synchronization Signal Blocks (SSBs) and Positioning Reference Signals (PRSs)—for monostatic sensing at base stations (BSs), leveraging existing infrastructure to efficiently enhance capabilities.

Given that sensing must coexist with communication in 5G systems, resource management is critical. It restricts available resources for sensing, thus limiting resolution. By fusing data from multiple BSs and processing it centrally, significant enhancements in sensing resolution are possible. This paper quantifies the resolution of monostatic and multi-monostatic BS systems by examining the spatial resolution area (SRA)—the region within which the system cannot differentiate between two objects—and localization resolution (LR), defined as the maximum distance error between a target's estimated and actual positions.

Our results show that in the FR1 band, using multiple monostatic BSs significantly enhances system resolution over a single BS setup. Adding a second BS improves SRA by at least 40 %. Employing larger bandwidths up to 100 MHz for PRSs achieves sub-1-meter LR with five BSs, while narrower bandwidths like 7.2 MHz for SSBs approach sub-10-meter LR with seven monostatic BSs.

Index Terms—3GPP, ISAC, monostatic sensing.

I. INTRODUCTION

Wireless sensing leverages radio frequency interactions with objects and human activity to detect environmental changes, offering extensive applications from drone intrusion detection to smart highways. Integrating wireless sensing into wireless networks through Integrated Sensing and Communication (ISAC) enhances spectral efficiency, optimizes resource use, and reduces hardware redundancy and network costs [1], [2].

The industry's growing interest in ISAC is driven by the potential for operators to offer more services using their existing networks. By integrating communication and sensing capabilities, they can enhance situational awareness and deliver personalized services while maintaining low operational costs. Reflecting this interest, the IEEE is developing the 802.11bf specification to incorporate sensing into Wireless Local Area Networks (WLANs), with finalization expected by 2025 [3], [4]. This marks a significant advancement in consumer wireless networks. Concurrently, the 3rd Generation Partnership Project (3GPP) is embedding sensing within its standards, with Release 19 introducing a technical report (TR) on supported use cases [5] and a sensing channel model.

Despite the ongoing standardization efforts, integrating sensing capabilities within 3GPP standards for 5G New Radio (NR) involves a complex and lengthy process that requires the development of new architectures, protocol operations, and deployment strategies. Operators must balance benefits against costs, which mandates practical and integrative approaches. One central design question is whether sensing should be supported at base station (BS) or user equipment (UE) level. BS-based sensing, which benefits from centralized processing, may require full-duplex systems and could incur higher costs. On the other hand, UE-based sensing allows for distributed data collection but necessitates hardware upgrades and more power. In the short term, sensing at the BS level is more feasible, as upgrades to BS infrastructure are generally simpler and less disruptive compared to the extensive modifications required for UEs. This approach not only avoids potential delays in adoption due to hardware compatibility issues and the logistical challenges of deploying new equipment to end users but also inherently supports the deployment of monostatic sensing solutions, where each BS can independently perform sensing tasks. Additionally, this approach supports the integration of data from multiple BSs, enhancing sensing performance through spatial diversity.

Leveraging existing 3GPP reference signals already transmitted by BSs offers a practical path for operators to adopt monostatic sensing with minimal infrastructure changes, reducing costs and easing deployment. Sensing can be implemented in either active or passive modes, each with its own trade-offs. Active sensing, which involves allocating dedicated resources for sensing, enhances sensing flexibility and performance but introduces additional communication overhead. In contrast, passive sensing relies on signals already in use for communication, incurring no extra overhead but with limited flexibility due to its dependence on existing signal timing. In this paper, we propose to repurpose Positioning Reference

Signals (PRSs)[1] for active sensing, taking advantage of their flexibility in resource allocation (timing and bandwidth), and Synchronization Signal Blocks (SSBs) for passive sensing, as they are already routinely transmitted for synchronization. This approach supports the deployment of monostatic and multi-monostatic BS configurations with minimal impact on network operation and a streamlined path to market for sensing-enabled networks.

Researchers have begun exploring sensing using BSs, including monostatic and multi-monostatic sensing resolution in 5G NR systems. For example, Pucci et al. [6] investigate BSs as monostatic radars using beam scanning for range and direction of arrival estimation. A promising strategy involves deploying multiple monostatic BSs and several studies [7]–[9] suggest that utilizing multiple BSs can improve detection accuracy through spatial diversity. However, these studies often overlook the costs of deploying multiple monostatic BSs, particularly the challenges of integrating them into a 3GPP-compliant architecture. Additionally, further studies demonstrate PRSs as effective for high-resolution sensing due to their long sequences and flexible time-frequency allocations [10], while SSBs provide a viable passive sensing option for moderate-resolution sensing [11].

The number of BSs used (monostatic or multi-monostatic configurations) and the choice of reference signals directly influence sensing resolution, impacting factors such as spatial diversity and and the frequency at which sensing measurements are performed. These elements underline the necessity for metrics to evaluate the achievable resolution of sensing systems comprehensively. In this study, we utilize two key resolution metrics: the Spatial Resolution Area (SRA) and Localization Resolution (LR). SRA is defined as the smallest area within which the system can distinguish between two distinct targets, reflecting the combined effect of range and angular resolution [12]–[14]. LR quantifies the largest potential spatial error in estimating a target's position within the SRA. Together, these metrics enable a comprehensive assessment of monostatic and multi-monostatic configurations, providing a clear, quantifiable measure of the overall sensing system resolution, independent of specific channel models or propagation effects.

The paper is structured as follows: Section II presents the system model for our 3GPP ISAC framework and in particular the practical integration of sensing capabilities and deployment strategies. Section III describes the geometrical modeling for monostatic sensing within 3GPP standards. Section IV evaluates the sensing resolution of our framework varying the bandwidths and number of monostatic BSs. Finally, Section V summarizes our findings, and outlines next steps for research.

II. ENABLING 3GPP SENSING

In this section, we introduce a system model that integrates sensing capabilities into the existing 3GPP framework using

---

[1]PRSs are specifically designed signals used for accurate location estimation and were introduced in 3GPP Release 16.
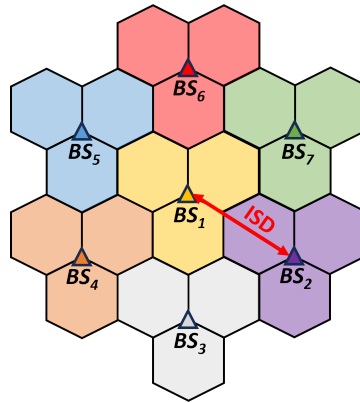

Fig. 1: Hexagonal grid layout for a 7-cell deployment scenario

monostatic BS sensing. This model capitalizes on SSBs and PRSs reference signals to conduct sensing tasks, aiming to minimize system complexity and optimize network resources. The study primarily focuses on the FR1 band, which remains prevalent in current communication networks. However, the methodology is equally applicable to the FR2 band.

The proposed system employs multiple monostatic BSs that serve both communication and sensing functions. These BSs are organized into a network layout consisting of seven sites, each configured into trisector hexagonal cells as illustrated in Fig. 1. This configuration positions BSs centrally within each cell and maintains consistent inter-site distances (ISDs) tailored for varied urban and rural settings. Specifically, the deployment spans Urban Micro (UMi) with an ISD of 200 m, Urban Macro (UMa) with an ISD of 500 m, and Rural Macro (RMa) with an ISD of 1732 m. Each BS functions independently as a monostatic sensing device, enabling the deployment of up to seven such devices. Thus, sensing information from up to all seven monostatic BSs can be fused together to enhance spatial diversity and improve overall system resolution.

A monostatic BS utilizes a co-located transmitter and receiver to detect targets by processing signals reflected off objects in the environment. We treat the target as a single-point in this study. Each BS is assumed to be equipped with full-duplex radios that support simultaneous transmission and reception on the same frequency band, enhancing operational efficiency. The BSs also feature uniform linear arrays (ULA) with N antenna elements, providing high angular resolution crucial for precise sensing operations. Additionally, the BSs are considered to be synchronized via the network backhaul, allowing for coordination in multi-monostatic scenarios.

The system utilizes SSBs or PRSs for sensing. SSBs, which are transmitted periodically at short intervals (e.g., tens of milliseconds), enable UEs to maintain continuous synchronization with the base station. SSBs are considered passive sensing signals as they are broadcast routinely for network operations. Their periodic nature allows for aggregation over multiple frames, extending their sensing coverage into neighboring cells and overcoming the usual cell-bound limits. The narrow

bandwidth of SSBs in FR1 (3.6 MHz or 7.2 MHz) limits their resolution, yet they remain suitable for passive detection tasks that do not demand high resolution

In contrast, PRSs are considered active sensing signals because they are used for the positioning function, a task distinct from standard communication processes in 3GPP systems. PRS offers configurable bandwidths of up to 100 MHz. This flexibility allows for finer range resolution, enabling more accurate detection and tracking of targets. The adjustable spatial and temporal resolution of PRSs makes them ideal for precise sensing tasks, such as object tracking or environmental mapping. By using both SSBs for moderately-demanding passive sensing and PRSs for high-resolution active sensing, the system adapts its capabilities depending on the specific application requirements.

III. MONOSTATIC AND MULTI-MONOSTATIC SENSING RESOLUTION MODELING

In this paper, we introduce a computational geometry-based approach to quantify the sensing resolution of monostatic BSs within typical 3GPP deployments. Our approach centers on two key metrics: the *SRA* and the *LR*. The SRA, defined as the smallest area, expressed in m^2, in which the system can resolve two distinct targets, reflects the uncertainty area in target localization. This area is influenced by both range resolution, dictated by the system's bandwidth, and angular resolution, determined by the beamwidth of the BS antenna array. Additionally, LR, expressed in m, quantifies the largest spatial error in estimating a target's position within the SRA. The LR provides a measure of the maximum potential error in pinpointing a target's location. Together, SRA and LR provide essential measures to evaluate and understand the fundamental limits of sensing accuracy.

A monostatic BS emits a signal and captures the reflections from objects in the environment. Processing the received signal enables us to obtain the range R, which is the distance between the system and the target, and given by $R = ct/2$, where t is the reflected signal's round trip time and c is the speed of light. The finite bandwidth B of the system defines the range resolution ΔR, introducing uncertainty in the estimated range with $\Delta R = c/(2B)$. This results in an uncertainty region—an annulus with width ΔR and area $U_A = \pi \cdot (R_{\max}^2 - R_{\min}^2)$, lying between the minimum and maximum possible ranges, $R_{\min}$ and $R_{\max}$, as depicted in Fig. 2.

Considering the angular resolution provided by a ULA with a finite beamwidth β radians, the beam's coverage area forms a wedge-shaped sector. The resulting uncertainty region from both range and beam resolutions is a polygon defined by the intersection of the beam wedge and the annulus, as shown in Fig. 2. The area of this polygon, U_A, is calculated as:

$$U_A = (\beta/2) \cdot (R_{\max}^2 - R_{\min}^2). \tag{1}$$

Let μ_R be the average range. We can write μ_R and ΔR as:

$$R_{\max} + R_{\min} = 2\mu_R, \tag{2a}$$
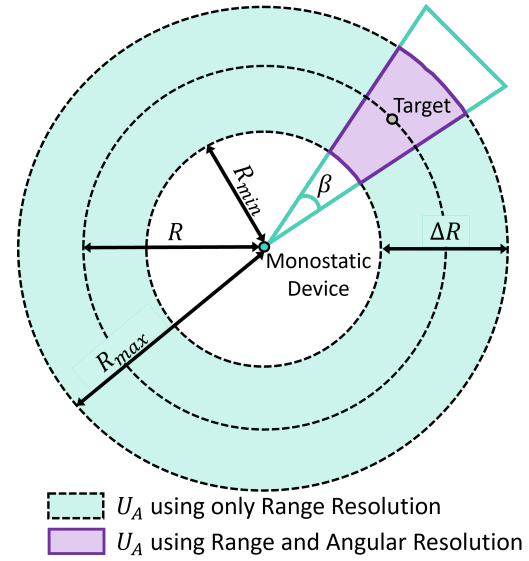$$R_{\max} - R_{\min} = \Delta R. \tag{2b}$$
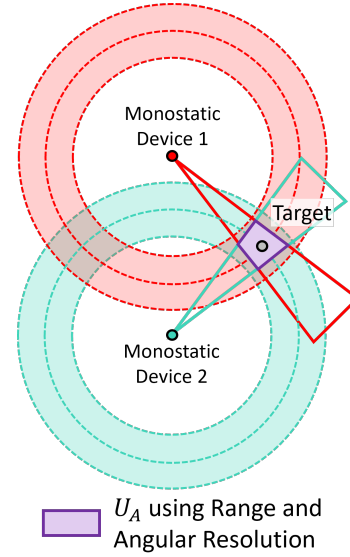

Fig. 2: Single monostatic device

Fig. 3: Two monostatic devices

Then, $R_{\max}^2 - R_{\min}^2 = 2\mu_R \cdot \Delta R$, and $U_A = \beta \cdot \mu_R \cdot \Delta R$.

In this study, the calculated U_A represents a specific instance of SRA under given sensing conditions, such as bandwidth and beamwidth. U_A illustrates the system's capacity to distinguish between closely spaced targets, setting the practical limits of spatial resolution based on $R_{\max}$, $R_{\min}$, and β. To evaluate the SRA, we calculate the U_A for various target positions in all cells, providing a system-wide perspective on resolution capabilities. Smaller SRA values indicate finer spatial resolution, supporting more precise target differentiation.

Simultaneously, we assess horizontal sensing accuracy H, defined in [5] as 'the closeness of the measured sensing result (i.e., position) of the target object to its true position value'. It measures the maximum spatial error in estimating a target's

position within the uncertainty area defined by U_A. H is obtained by calculating the maximum distance $d_{\max}$ from the centroid of U_A to its vertices, representing the largest possible deviation from the true position of the target. This value serves as an upper bound on localization accuracy, where a smaller H indicates a higher precision in target localization. To evaluate LR across the network, we compute H for multiple target positions in each cell, providing a comprehensive view of the system's localization accuracy under various configurations.
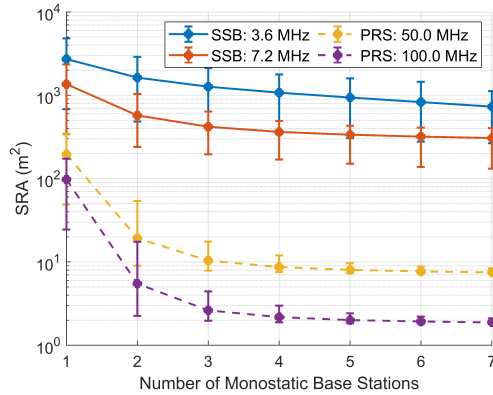
In this study, we investigate the use of multi-monostatic BSs to enhance sensing resolution in 3GPP deployments. As illustrated in Fig. 3, deploying several BSs allows their respective U_A to intersect, effectively narrowing the overall U_A and thus improving both the SRA and LR. This intersection represents the fusion of sensing information at a central entity. By employing computational geometry to systematically calculate the intersection of these polygons, we can quantify the overall sensing resolution and assess how various BS configurations and placements affect it.

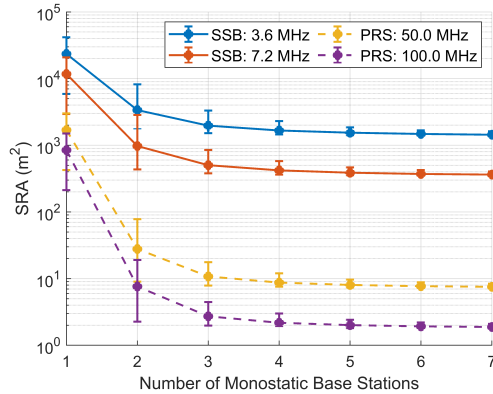## IV. SENSING RESOLUTION EVALUATION

In this section, we evaluate the SRA and LR of the sensing system based on the system's design parameters (bandwidth and beamwidth) using U_A and H metrics obtained through the computational-geometry methodology described in Section III. Operating in the FR1 band within a 3GPP deployment, the system covers 7 sites, as outlined in Section II. We examine 2200 target locations uniformly distributed across these cells to assess how SRA and LR change with the number of monostatic BSs (N_{BS}), ranging from 1 to 7[2]. For reference signals, SSBs, configured to their FR1 bandwidth values of 3.6 MHz or 7.2 MHz, use either 4 or 8 directional beams corresponding to transmission beamwidths of 15 degrees and 30 degrees. In our assessments, a 15-degree beamwidth serves as a representative value. For PRSs, we explore bandwidths of 50 MHz and 100 MHz, where the latter enables full FR1 band usage to enhance sensing resolution, while the former reserves half of the bandwidth for communication when PRSs are transmitted to study trade-offs between sensing and communication efficiency. The SRA and LR represent the overall resolution of the system deployment, characterized by the mean values of U_A and H, respectively, which are calculated across the 2200 target locations. Figures 4 and 5 display the SRA and LR for both UMi and RMa deployments[3], along with the 5th and 95th percentiles to illustrate variability and robustness across different scenarios.

A. Effect of reference signal bandwidth

A central observation of our analysis is that increased bandwidth leads to a reduction in the SRA values, as evidenced in Fig. 4. Larger bandwidth settings, such as the 50 MHz

---

[2]Note that configurations with fewer than 7 BSs offer multiple arrangement possibilities (e.g., with two BSs, 21 different combinations are feasible)

[3]Results for UMa are omitted due to space constraints; however, trends are consistent.

(a) UMi: ISD = 200 m

(b) RMa: ISD = 1732 m

Fig. 4: SRA with 5th and 95th percentile values

and 100 MHz used in PRSs configurations, result in significantly smaller SRA compared to the SSBs configurations. A smaller SRA indicates that the system is more capable of discriminating between closely situated targets, enhancing the overall spatial resolution. This improvement is attributed to the enhanced range resolution afforded by higher bandwidth, which effectively diminishes the SRA. This correlation is similarly reflected in Fig. 5, where larger PRS bandwidths correspond to a smaller LR. Smaller values of LR indicate higher accuracy in pinpointing a target's exact position within the uncertainty area, enhancing the system's localization capabilities. While PRSs provide superior resolutions due to their larger bandwidth, the trade-off includes increased communication overhead from active sensing. Conversely, SSBs-based sensing leverages already transmitted signals (passive sensing), incurring no additional overhead but at the cost of reduced localization precision. Consequently, PRSs are more suited for applications demanding high resolution, while SSBs are adequate for applications with less stringent resolution requirements.

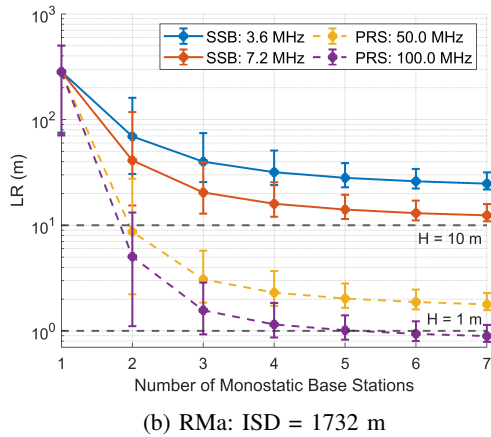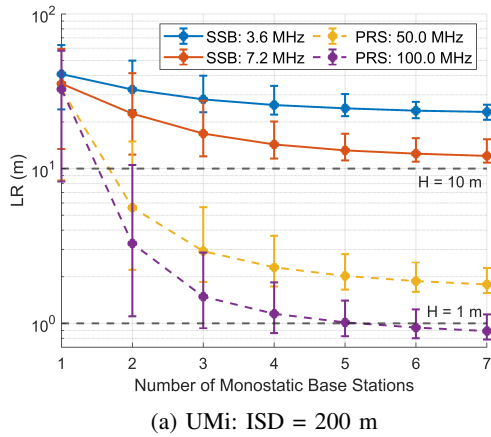(a) UMi: ISD = 200 m

(b) RMa: ISD = 1732 m

Fig. 5: LR with 5th and 95th percentile values

B. Effect of deployment density and number of monostatic BSs

Observations from Fig. 4 indicate that the SRA is affected by the density of the deployment environment. Specifically, the SRA values are larger in the sparser (RMa) deployment than in the UMi deployment, as illustrated in Fig. 4b compared to Fig. 4a. A similar trend is observed for LR in Fig. 5. However, we can observe that the larger the bandwidth and the number of BSs, the smaller the differences between the two deployments, suggesting that increasing both bandwidth and BS count can effectively reduce the disparities in sensing resolution between denser and sparser environments.

From Fig. 4, we can observe that deploying a single BS results in the largest SRA. Introducing additional monostatic BSs generally lowers the SRA, demonstrating the benefits of a multi-monostatic system regarding spatial resolution. The inclusion of a second BS typically at least halves the SRA (the only exception being 40 % for SSB 3.6 MHz), marking the most substantial improvement by increasing the overlap of uncertainty areas. However, as the number of BSs increases, the rate of improvement in reducing the SRA diminishes, reflecting diminishing returns with each additional BS added. Similar trends are observed for LR, as illustrated in Fig. 5.
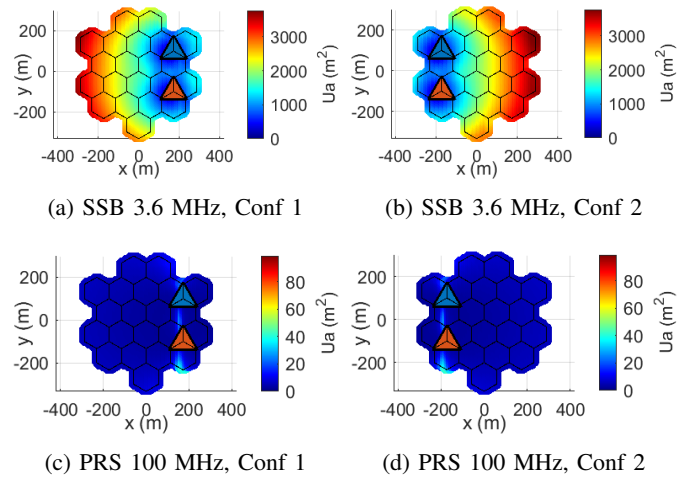

(a) SSB 3.6 MHz, Conf 1

(b) SSB 3.6 MHz, Conf 2

(c) PRS 100 MHz, Conf 1

(d) PRS 100 MHz, Conf 2

Fig. 6: Visualization of all U_A for 2 monostatic BSs configurations and UMi deployment (the BSs are the triangle markers)

According to [5], different applications require varying levels of horizontal accuracy, ranging from 1 m for critical applications like railway intrusion detection to 10 m for general applications like smart home security. PRS configurations at 100 MHz bandwidth achieve sub-1 m LR when more than four BSs are used, suitable for high-precision applications. In contrast, SSBs do not achieve sub-10 m accuracy, with SSB 7.2 MHz at 7 BSs nearing this threshold (12.08 m and 12.38 m for UMi and RMa, respectively). However, SSB-based sensing remains suitable for less demanding tasks. For example, using SSB 3.6 MHz with $N_{BS} = 3$ yields a LR of 20.4 m in the UMi case, which does not meet the 10 m accuracy standard but suffices for non-critical applications and without any additional overhead. The optimal performance is observed with PRS at 100 MHz in a UMi deployment with $N_{BS} = 7$, achieving a SRA of less than 2 m^2 and a LR of approximately 0.89 m. A 50 MHz PRS configuration, while allocating half the bandwidth for communication, still achieves solid sensing resolution, yielding an SRA of 7.5 m^2 and an LR of approximately 1.7 m. Generally, adding more than three BSs does not significantly enhance LR; for example, the reduction in LR is less than 9 % by adding a fourth BS in SSB-based sensing for the UMi deployment. In summary, both UMi and RMa deployments benefit from the strategic addition of monostatic BSs and deploying up to three BSs appears optimal for balancing resolution improvements against complexity and cost.

C. Effect of the BSs selection

We investigate the impact of BS selection on sensing resolution by examining the spatial distribution of each individual U_A, as visualized in Fig. 6. This figure displays the 2200 target position U_A values across two distinct bandwidths and two selected configurations from the 21 possible when employing two monostatic BSs out of a set of seven. Specifically, Figs. 6a and 6b demonstrate configurations using SSBs at a 3.6 MHz

bandwidth, while Figs. 6c and 6d utilize PRSs at a 100 MHz bandwidth. These configurations are chosen to highlight the influence of BS locations on the distribution of U_A. A critical observation from Figs. 6a and 6b is that BS selection markedly affects the spatial distribution of U_A. In both configurations, larger U_A (exceeding 3000 m^2) are mainly found at locations opposite to the BSs, underscoring the significance of strategic BS placement and selection, based on the specific area to monitor, especially when operating with SSBs lower bandwidths.

Using larger bandwidths, as permitted by PRS, improves sensing resolution, as shown in Figs. 6c and 6d. With a 100 MHz PRS setting, the SRA values consistently remain below 100 m^2. For instance, at the coordinates $x = 200\ m$ and $y = 150\ m$, U_A reduces to 10.6 m^2 in configuration 1 and further to 4.6 m^2 in configuration 2, compared to 3162.6 m^2 under a 3.6 MHz SSB setting in configuration 2. The improvement from increasing bandwidth is significant, as expected, but even with the largest bandwidth, the SRA in configuration 1 is still twice that of configuration 2. This underscores the necessity for BS selection mechanisms, even at higher bandwidths, to achieve optimal resolution for given monitoring region.

D. Results Insights

Our findings highlight the significant impact of operational parameters on the sensing resolution. Bandwidth emerges as a pivotal factor; higher bandwidths, such as 100 MHz in PRS-based configurations, substantially enhance both SRA and LR. This improvement is crucial for applications requiring high resolution, like traffic management and emergency response. Conversely, lower bandwidths, such as the one offered by SSBs, are more economical and overhead-free as they operate passively, offering reduced resolution suitable for less demanding applications such as smart home settings

Deployment density and the number of monostatic BSs also significantly influence sensing resolution. Sparser deployments typically show larger SRA and LR, though increasing bandwidth and BS count can reduce these differences. However, increasing the number of BSs provides diminishing returns, with the addition of a second BS producing the most substantial resolution improvement, while gains decrease beyond three BSs, highlighting an optimal balance between performance and complexity. Finally, strategic BS selection tailored to the monitoring region is essential for achieving targeted resolution.

Given these observations, operators might benefit from a phased approach to bandwidth enhancement, beginning with lower bandwidths to manage initial costs and meet basic requirements, then gradually increasing as demands grow. This strategy not only progressively enhances sensing resolution but also optimizes resource use and cost efficiency. Alongside this, designing effective BS selection mechanisms and carefully calibrating the number of BSs, especially in sparse deployments, will be crucial for achieving the desired sensing performance.

V. Conclusion

This paper explores the integration of sensing capabilities in 5G NR using monostatic BSs and applies a computational geometry approach to quantify the sensing resolution achieved through reference signals. Passive SSB configurations, which are overhead-free, provide an economical option for moderate accuracy needs, while active, higher-bandwidth PRS setups are ideal for high-precision applications due to their enhanced resolution. Additionally, we show that effective BS selection and phased bandwidth enhancements will be key for operators to optimize performance and manage costs. Future work will investigate the effects of transmit power and propagation on sensing resolution.

References

[1] A. Kaushik, R. Singh, S. Dayarathna, R. Senanayake, M. Di Renzo, M. Dajer, H. Ji, Y. Kim, V. Sciancalepore, A. Zappone, and W. Shin, "Toward integrated sensing and communications for 6G: Key enabling technologies, standardization, and challenges," *IEEE Communications Standards Magazine*, vol. 8, no. 2, pp. 52–59, 2024.

[2] J. Wang, N. Varshney, C. Gentile, S. Blandino, J. Chuang, and N. Golmie, "Integrated sensing and communication: Enabling techniques, applications, tools and data sets, standardization, and future directions," *IEEE Internet of Things Journal*, vol. 9, no. 23, pp. 23416–23440, 2022.

[3] T. Ropitault, C. R. C. M. da Silva, S. Blandino, A. Sahoo, N. Golmie, K. Yoon, C. Aldana, and C. Hu, "IEEE 802.11bf WLAN sensing procedure: Enabling the widespread adoption of WiFi sensing," *IEEE Communications Standards Magazine*, vol. 8, no. 1, pp. 58–64, 2024.

[4] S. Blandino, T. Ropitault, C. R. C. M. da Silva, A. Sahoo, and N. Golmie, "IEEE 802.11bf DMG sensing: Enabling high-resolution mmWave Wi-Fi sensing," *IEEE Open Journal of Vehicular Technology*, vol. 4, pp. 342–355, 2023.

[5] "Feasibility study on integrated sensing and communication," Tech. Rep. TR 22.837, 3rd Generation Partnership Project (3GPP), Online, 2024. Accessed: 2024-09-23.

[6] L. Pucci, E. Paolini, and A. Giorgetti, "System-level analysis of joint sensing and communication based on 5G new radio," *IEEE Journal on Selected Areas in Communications*, vol. 40, no. 7, pp. 2043–2055, 2022.

[7] S. Mandelli, M. Henninger, M. Bauhofer, and T. Wild, "Survey on integrated sensing and communication performance modeling and use cases feasibility," in *2023 2nd International Conference on 6G Networking (6GNet)*, pp. 1–8, 2023.

[8] M. R. Figueroa, P. K. Bishoyi, and M. Petrova, "Cooperative multi-monostatic sensing for object localization in 6G networks," in *2024 IEEE Wireless Communications and Networking Conference (WCNC)*, pp. 1–6, IEEE, 2024.

[9] X.-T. Meng, B.-X. Cao, F.-G. Yan, M. Jin, and Y. Zhang, "Target localization for monostatic MIMO radar based on a double polynomial rooting technique," *IEEE Communications Letters*, vol. 26, no. 2, pp. 454–457, 2021.

[10] Z. Wei, Y. Wang, L. Ma, S. Yang, Z. Feng, C. Pan, Q. Zhang, Y. Wang, H. Wu, and P. Zhang, "5G PRS-based sensing: A sensing reference signal approach for joint sensing and communication system," *IEEE Transactions on Vehicular Technology*, vol. 72, no. 3, pp. 3250–3263, 2023.

[11] K. Abratkiewicz, A. Księżyk, M. Płotka, P. Samczyński, J. Wszołek, and T. P. Zieliński, "SSB-based signal processing for passive radar using a 5G network," *IEEE Journal of Selected Topics in Applied Earth Observations and Remote Sensing*, vol. 16, pp. 3469–3484, 2023.

[12] S. R. Doughty, *Development and performance evaluation of a multistatic radar system*. University of London, University College London (United Kingdom), 2008.

[13] M. M. Weiner and P. D. Kaplan, "Bistatic surface clutter resolution area at small grazing angles," tech. rep., The MITRE Corporation, 1982.

[14] M. M. Weiner, *Advances in Bistatic Radar*, ch. 9, pp. 230 – 319. Scitech Publishing, 2007.